

Highly Uniform Nanodiamond-Graphene Composites Microspheres for Electrocatalytic Hydrogen Evolution

Ibrahim K. Alsulami,* Shittu Abdullahi,* Ahmed Alshahrie, Thaar M. D. Alharbi, Mohammed Alahmadi, Sami B. E. N. Aoun, and Numan Salah*



Cite This: *ACS Omega* 2024, 9, 17808–17816



Read Online

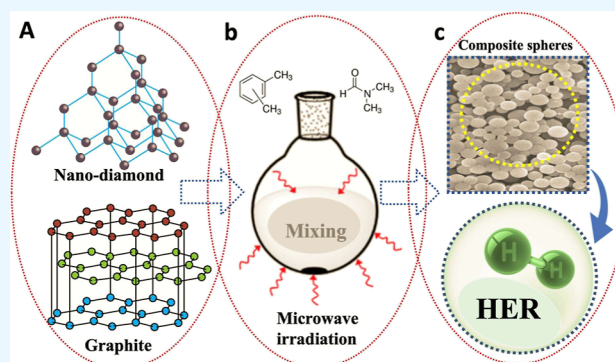
ACCESS |

Metrics & More

Article Recommendations

Supporting Information

ABSTRACT: To progress the clean hydrogen-gas-based energy economy, there is a demand for cost-effective, highly efficient catalysts to facilitate the hydrogen evolution reaction process (HER). Due to the amazing catalytic capabilities of two-dimensional materials, extensive research has been done on these structures. However, most of the described syntheses take a lot of time, are challenging, and are ineffective. The present work demonstrates the performance of the recently reported nanodiamond/graphene composite microsphere ND-GCSs as a catalyst for HER. These spheres were produced via the microwave-irradiation approach. A modified process was adopted to improve the particle size uniformity and yield. The prepared composite spheres showed very interesting catalytic activity for the HER when assembled on a screen-printed carbon electrode. The prepared ND-GCSs@SPCE showed a significant shift of the onset potential to ca. -450 mV and a small Tafel slope value of ca. 85 mV/decade. The electron transfer was drastically enhanced with a tremendous decrease in charge transfer resistance to ca. 265 Ω . The electrocatalyst showed excellent long-term stability for the HER application. Additionally, this novel composite structure might be beneficial for diverse applications including batteries, supercapacitors, catalyst supports, and more.



1. INTRODUCTION

Within the framework of a sustainable energy system emphasizing cleanliness and environmental consciousness, where conventional fossil fuels are scarce and the demand for renewable energy is high, the concept of hydrogen evolution as an energy storage solution has garnered considerable attention.^{1,2} Numerous potential sources, such as coal, biomass, pollutants removal from wastewater, water electrolysis, photoelectrochemical water splitting, and electrochemical methods, offer pathways for hydrogen production.^{3,4} While platinum (Pt) and Pt-based materials stand out as the most renowned electro-catalysts for hydrogen/oxygen energy systems due to their remarkable efficiency, they are also exceedingly expensive and rare on Earth.^{5,6} Consequently, researchers have been actively seeking affordable and readily available alternatives to noble materials, capable of serving as effective catalyst substitutes across various applications involving hydrogen and other energy forms.^{7,8}

Lately, numerous initiatives are carried out to combat and substitute the noble metals with earth-abundant transition metals for active HER performance, such as molybdenum, tungsten, nickel, and cobalt.⁹ Other oxide and sulfide materials¹⁰ in nanostructure forms are currently employed as a substitute for the Pt-electrode to be applied in energy and storage applications. The novel electrode materials derived

from layered transition chalcogenides (metals) represent a promising avenue for energy storage applications.¹¹ Extensive research has demonstrated their effectiveness in various fields, including hydrogen evolution reactions (HER), rechargeable lithium batteries, and supercapacitors. Nanomaterials such as ZnS, Ni₃S, CoS₂, CuS, and Bi₂S₃ have particularly shown significant potential in enhancing the performance and efficiency of these energy storage systems.^{12,13}

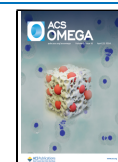
Hydrogen (H₂) is a promising alternative energy due to its high energy density and low carbon emissions, making it a crucial solution for replacing depleting natural resources and addressing environmental concerns.¹⁴ The water-splitting electrochemical process, which produces clean hydrogen fuel, is an efficient and environmentally friendly method of storing renewable energy.¹⁵ In the electrocatalytic water-splitting process, the HER and the oxygen evolution reaction constitute the two essential half-cell processes.¹⁶ Even though platinum metals and platinum-based materials are the most effective

Received: September 5, 2023

Revised: April 1, 2024

Accepted: April 4, 2024

Published: April 13, 2024



HER catalysts, their use is limited due to their high cost and scarcity.¹⁷ Carbon-based materials, such as graphene, have been identified as among the most promising catalysts for boosting HER performance due to their unique structures (high surface area) and chemical and physical characteristics.¹⁸

Besides shape, another crucial factor influencing the electrocatalytic performance of HER catalysts is their electrical conductivity. Carbon materials like graphene, carbon nanotubes (CNTs), reduced graphene oxide, and more possess distinctive properties that are considered when selecting the most suitable supports to enhance electrocatalytic activity. The hexagonal lattice structure composed of interconnected two-dimensional (2D) sheets of sp²-bonded carbon atoms in graphene showcases outstanding features, such as swift charge carrier mobility, superior electrical conductivity, and an exceptionally vast specific surface area.^{19,20} Consequently, graphene of different types has been examined as conductive supports for diverse materials, such as MoS₂ catalysts, to demonstrate elevated HER electrocatalytic performance.²¹

Many techniques for producing these hybrid materials suffer from drawbacks related to safety, scalability, and cost as well as sophisticated setups, extended synthesis durations, and high utilization of energy. These limitations curtail their potential applications. For instance, methods involving hazardous gases including calcination in an H₂/Ar atmosphere,²¹ prolonged precursor materials heating,^{21,22} intricate lyophilization dehydration processes,²³ labor-intensive electrodeposition requiring specialized handling, among others, present significant challenges. In this context, microwave irradiation emerges as a promising method for fabricating efficient catalysts for the HER. Presently, the research domain involving synthetic chemistry using microwave irradiation is rapidly expanding, owing to its rapid volumetric heating, enhanced reaction rates, improved selectivity, reduced reaction times, and increased product yields.²³

The method of microwave irradiation has proven to be successful in producing various hybrid compounds, particularly in synthesizing composite carbon nanomaterials of diverse shapes and sizes. This effectiveness stems from the exceptional radio-absorbing properties of carbon-rich materials.²⁴ Through the absorption of microwave radiation, these materials efficiently produce rapid heat, enabling a variety of chemical processes.²⁵ Carbon materials synthesized via microwave irradiation have been extensively studied for diverse applications.²⁴

Previous research has investigated combining nanodiamonds with graphene or graphite for various applications.^{26,27} Diamond nanoparticles have been used to enhance graphene exfoliation²⁸ and reduce friction.^{29,30} However, there's a limited exploration of using diamond nanoparticles for graphene exfoliation or converting graphite into ND-GCSs carbon microspheres under microwave irradiation.^{31,32} Additionally, to the best of the authors' knowledge, no study in the open literature has reported on the potential use of ND-Gr composites as active catalysts for the hydrogen evolution reaction (HER).

In this study, we explored the potential application of the generated ND-GCSs for the electrocatalytic hydrogen evolution reaction (HER). Consistent with previous findings,^{31,32} diamond nanoparticles were discovered to be remarkably efficient in exfoliating and transforming graphite layers into exceptionally uniform ND-GCSs using microwave irradiation, without the need for surfactants or additional

auxiliary substances. Therefore, the testing of such ND-GCSs microspheres for the electrocatalytic HER might be the ultimate choice for this application. The synthesized ND-GCSs, produced in a modified process, were further characterized after their improvement by using numerous well-known techniques. This modification of the process was adopted to improve the particle size uniformity and yield. Additionally, here we have demonstrated that microwave can prepare larger quantities of the ND-GCSs for the two mixing solutions in record time; this capability can be further extended by increasing the liquid volume. Then these ND-GCSs were assembled on a screen-printed carbon electrode (SPCE) and evaluated as catalysts for the HER. The long-term stability of the electrocatalyst was examined by cyclic voltammetry (CV). The obtained results were discussed in more detail.

2. METHODOLOGY DETAILS

2.1. Materials. Graphite flakes of 99.5% purity were acquired from AD Nanotech, Co. in India, while spherical diamond nanoparticles (ND) with a purity exceeding 98% were sourced from Nanostructured & Amorphous Materials, Inc. in the USA. The ND utilized in this study were synthesized through the explosion technique, with an average particle size ranging from 3 to 10 nm, as detailed by the manufacturer (<https://www.nanoamor.com/inc/sdetail/14157>). These powders were, respectively, designated as graphite-rec and NDs-rec upon receipt. The solvents employed, dimethylformamide (DMF) and xylene, boasting a purity of 99.5% were supplied by Sigma-Aldrich in Germany.

2.2. Synthesis of the ND-GCSs. Uniform spherical structures, formed through a combination of graphene (Gr) and nanodiamond (ND) particles, were generated using a microwave chemical-assisted method employing a Milestone microwave oven system from Italy, similar to previous reports³² but with process modifications. Given graphene's tendency for poor dispersion and strong layer stacking interactions limiting its utility, high-power ultrasonication was employed as an effective exfoliation method to potentially yield monolayer or few-layer graphene at elevated concentrations. Acoustically treated graphene layers were utilized to facilitate the formation of uniform spheres with a consistent size and shape.

To begin, the graphite flakes were suspended in dimethylformamide (DMF) at a concentration of 100 mg/mL and subjected to ultrasonication for 15 min at approximately 250 W using a Hielscher Ultrasound Technology UIP500 HDT generator. Subsequently, the solution underwent centrifugation for 20 min at 4000 rpm to eliminate remnants of graphite flakes, followed by a filtration process with a filter paper of pore size of around ~80 nm before mixing with nanodiamond particles.

Nanodiamond particles mixed in pure xylene solutions were added at varying concentrations of 5 mg/mL corresponding to 5% graphene solution, 10 (10%), 15 (15%), and 20 mg/mL (20%), respectively. The diamond nanoparticles within the xylene solution were then dispersed for 20 min in a water bath sonicator before centrifuging the solution for 20 min at 4000 rpm to eliminate the remnant particles. After that, the solution containing the graphene and the other containing the diamond nanoparticles were combined within a glass flask of 1000 mL and mixed using a magnetic stirrer for 60 min at room temperature.

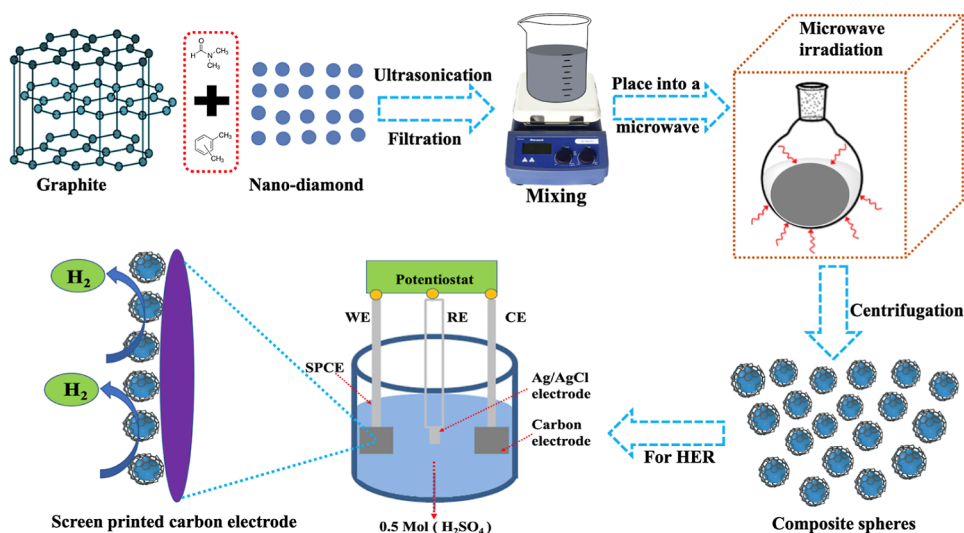


Figure 1. Microwave-irradiation synthesis process of nanodiamond-graphene composite spheres (ND-GCSs), utilized as an electrocatalyst for the HER.

The mixture was then subjected to microwave radiation in a microwave oven equipped with a display screen for monitoring the reaction parameters, a magnetic stirrer to maintain the homogeneity of the mixture during irradiation, and a condenser. The mixture was irradiated at 1000 W for different irradiation times such as 5, 10, 15, 20, and 30 min, respectively, while retaining approximately the same temperature of 135 °C during the irradiation. Thereafter, the mixture was allowed to cool before subjecting to a centrifuge at 4000 rpm for 20 min to eliminate the remaining undispersed particles. They were then washed repeatedly with pure ethanol and double-deionized water. The fabricated spheres were stored in an oven at 80 °C for 24 h for characterization.

2.3. Sample Characterizations. As detailed in a prior experimental report,³² various complementary techniques were utilized to characterize the morphological structure to determine the shape and size of the composite spheres, and the chemical composition of the newly synthesized material, as well as its properties. Similarly, in this study, these techniques included field emission scanning electron microscopy, utilizing a JEM 6700F from JEOL, Japan. X-ray diffraction (XRD) analysis was conducted with a ULTIMA IV instrument from Rigaku, Japan, using Cu K α radiation ($\lambda = 1.5406 \text{ \AA}$) at a fixed voltage of 40 kV and a current of 20 mA. Additional parameters of the XRD recording system included a grazing incidence angle of 1°, a step size of 0.02°, and a 2θ recording range of 5–90°. Raman spectroscopy was performed with a DXR Raman microscope from Thermo Scientific, USA, employing an excitation laser source set at 532 nm with a power of 6 mW. Fourier transform infrared spectroscopy (FTIR) was conducted using an FTIR (Nicolet iS10) instrument from Thermo Fisher Scientific, USA, employing the attenuated total reflectance technique. X-ray photoelectron spectroscopy (XPS) analysis was performed with a PHI 5000 Versa Probe model from PHI, Japan, capturing both narrow and survey spectra. Additionally, the elemental composition of the uniform ND-GCSs was investigated using a Horiba scientific ULTIMA-2 model of Inductively Coupled Plasma-Optical Spectrometer.

2.4. Electrochemical Investigation. An Autolab PGSTAT204 system was employed to conduct and regulate

all electrochemical experiments. A disposable three-electrode configuration consisting of a SPCE from Metrohm was utilized, with carbon, Ag/AgCl, and carbon serving as the working standard and counter electrodes, respectively. All electrochemical analyses were performed at ambient temperature under a high-purity nitrogen atmosphere. Sulfuric acid (H_2SO_4 , 0.5 M, pH = 0) was employed as the electrolyte for all experiments.

In a typical procedure, 100 mg of the ND-GCSs composite microspheres produced were dispersed in 1 mL of a 1:3 water/isopropanol solution. The ND-GCSs catalyst ink was sonicated for 1 h to ensure homogeneous dispersion. Subsequently, a well-dispersed catalyst solution of 2 μL was drop-cast on the working carbon electrode (4 mm diameter) and allowed to dry naturally. Finally, the working surface area was coated with 2 μL of Nafion solution (1:3 water/propanol) to prepare the ND-GCSs@SPCE electrocatalyst.

Linear sweep voltammetry (LSV) was employed to monitor the hydrogen evolution reaction (HER) in N_2 -saturated 0.5 M H_2SO_4 by sweeping the potential from 0.2 to -0.8 V at a scan rate of 1 mV/s. All potentials in this study are reported in the reversible hydrogen electrode scale using eq 1. Electrochemical impedance spectroscopy (EIS) analysis was conducted by applying a single-sine perturbation wave with an amplitude of 10 mV and a 125 ms integration time at -0.6 V over a frequency range from 50 kHz to 0.1 Hz. The long-term stability of the electrocatalyst was assessed via CV performed between 0.2 and -0.8 V at a scan rate of 100 mV/s.

$$E_{\text{RHE}} = E_{\text{Ag/AgCl}} + 0.1976 + 0.056\text{pH} \quad (1)$$

3. RESULTS AND DISCUSSION

3.1. Characterization of the Optimized ND-GCSs Composite Microspheres. In this study, we showcase the direct growth of ND-GCSs using a straightforward, scalable, and efficient microwave-irradiation method, as illustrated in Figure 1. The ND-GCSs composite microspheres were thoroughly characterized, and the results are depicted in Figure 2c,d. Additionally, numerous electrochemical experiments were conducted to assess the improved catalytic activities of ND-GCSs toward the hydrogen evolution reaction

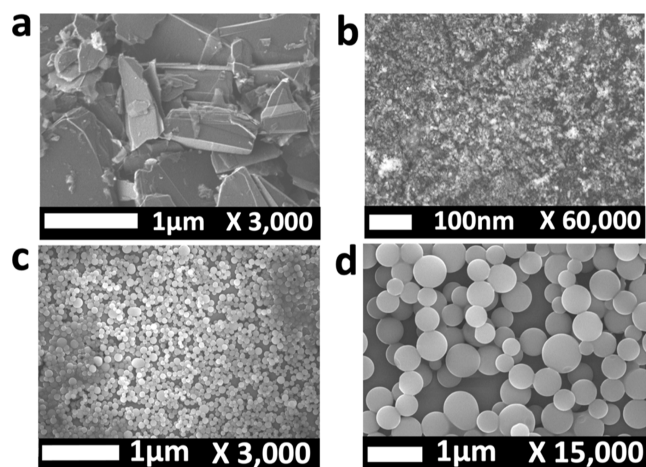


Figure 2. SEM images depicting the pure-graphene and pure-ND samples in (a,b), respectively. In (c,d), SEM images at a different magnification showcase the ND-GCSs generated through microwave irradiation, utilizing a 1:1 ratio of xylene and DMF as the solvents.

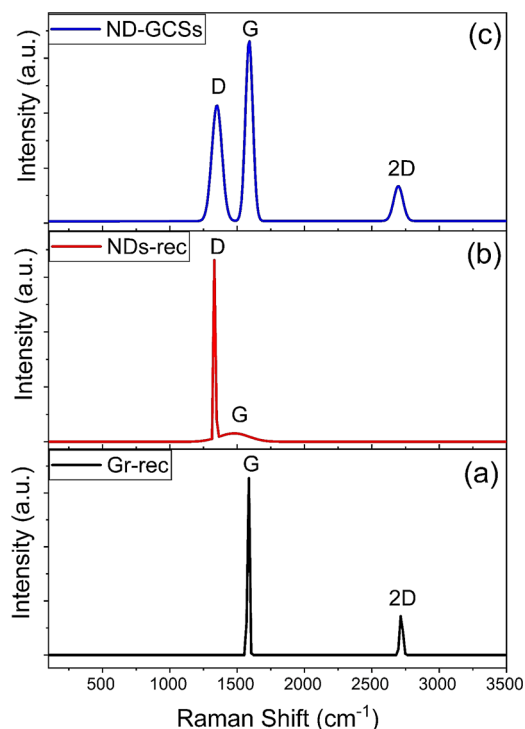


Figure 3. Raman spectra of Gr-rec (a), ND-rec (b), and optimized ND-GCSs (c).

(HER). As described earlier in previous experiments,³² it has been attempted to control the composite spheres' size, shape, and morphology by varying experimental parameters including the absence of one solvent (DMF or xylene), changing the reaction time, and the absence of NDs itself. This was accomplished without the addition of any other reagents, achieving a notable quantitative yield of 94%. It is found that most such changes do not affect the spherical size, shape, or morphology; only a single specific experimental setting parameter with its formulated ingredient can perform a substantial change to spherical morphology and size. Therefore, in this scientific report, we have followed the exact procedure performed in the previously published paper,³² but

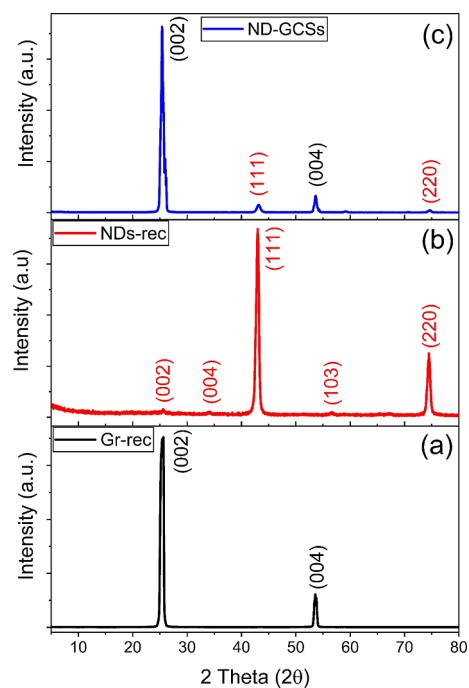


Figure 4. XRD patterns of Gr-rec (a), ND-rec (b), and optimized ND-GCSs (c).

with some modifications in the process to enhance the final structure, and the outcome was used to study the electrochemical performance of the prepared ND-GCSs toward the electrocatalysis of HER.

Here in this work, the high-power ultrasonication method plays a significant role in the exfoliation of the graphene layers into multiple and few layers of graphene as well as facilitating the process of wrapping the exfoliated layers around the diamond particles. A significant transformation in the structure including the size and the shape was observed prior to and after employing the ultrasonication method, as illustrated in Figure S3 (Supporting Information). The extracted graphene layers from the graphite flakes underwent successful conversion into a uniform spherical shape without any aggregation during ultrasonication and microwave irradiation, as depicted in Figure 2a–d. Notably, without employing the ultrasonication method, a spherical shape was evident, albeit with fragments of exfoliated layers of graphene, as demonstrated in Figure S1 (Supporting Information).

In Figure 2a, the pristine graphite sample exhibits surface flakes characterized by irregular shapes and sizes, ranging from 5.5 μm . Conversely, Figure 2b showcases the pristine ND sample, distinguished by its markedly smaller dimensions ranging between 5 and 10 nm, displaying spherical configurations. The morphological transformation of the optimized structure is depicted in Figure 2c,d, respectively.

During this optimization process, a constant microwave power of 1000 W was maintained for 30 min, resulting in a temperature of approximately 135 $^{\circ}\text{C}$. The graphene concentration in DMF was standardized at 100 mg/mL, while the diamond nanoparticles concentration in xylene stood at 5 mg/mL, constituting a graphene concentration of 5%. The initial solvent ratio of xylene to DMF in the microwave digester flask was upheld at 1:1, a choice guided by a prior investigation³¹ which demonstrated favorable outcomes with this solvent combination. It is worth noting that adjustments in

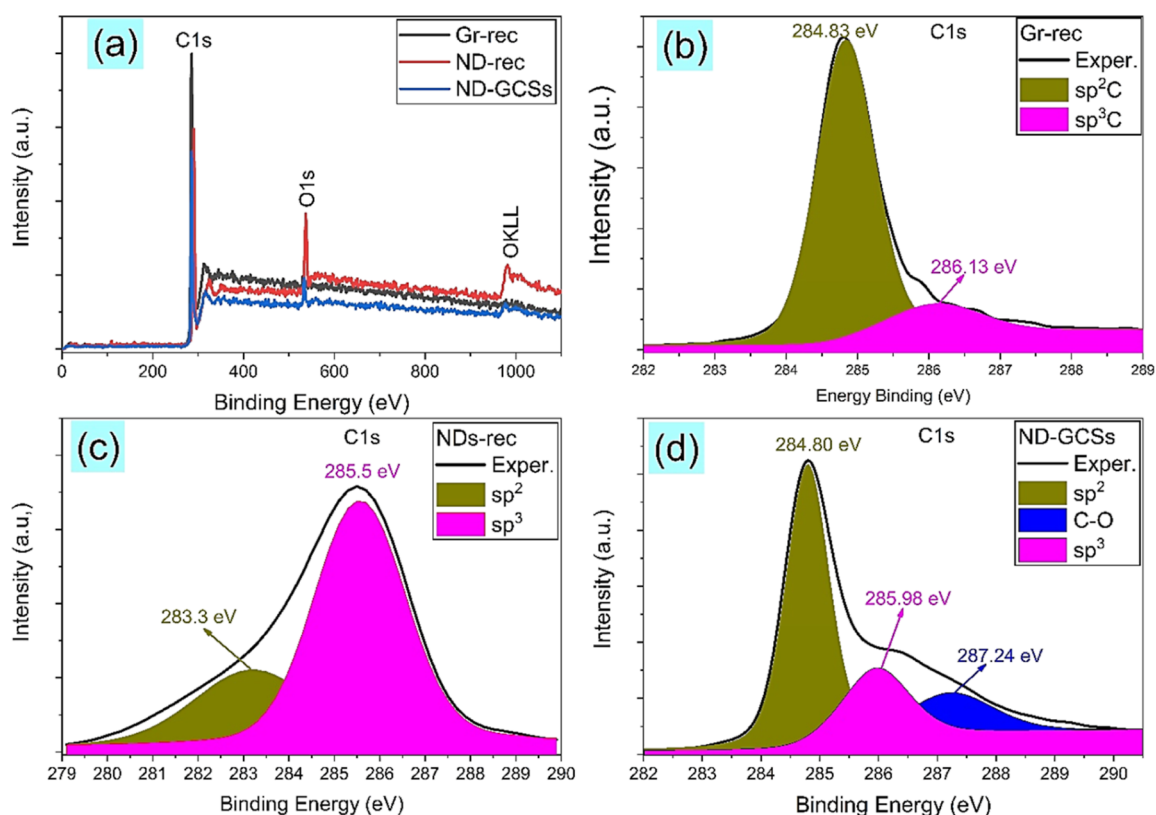


Figure 5. XPS patterns of (a) all of the samples under study, (b) Gr-rec, (c) ND-rec, and (d) optimized ND-GCSs.

exposure time, utilization of either xylene or DMF exclusively, or variations in ND concentration have the potential to alter the ND-GCSs structure. Furthermore, the exclusion of either solvent during the procedure impedes the formation of a distinct spherical structure, as illustrated in Figure S2 (Supporting Information).

Figures 2c,d and S1 (Supporting Information) showcase the outcome of blending these two carbon materials under the optimized conditions detailed above. A noticeable transformation in structure is evident prior to microwave irradiation and after the procedure. Remarkably, all graphene layers from the graphite flakes were converted into uniform spherical shapes without aggregation when mixed with the diamond nanoparticles. These images vividly illustrate the efficient conversion of multilayer graphite into highly uniform spherical structures with a high yield, and smooth surfaces, devoid of aggregation, following mixing with a small quantity of ND (specifically 5% of the graphene concentration). The subsequent ND-GCSs composite spheres exhibit highly smooth surfaces with a size ranging from approximately 0.4–1.2 μm .

Furthermore, BET analysis was conducted on the optimized ND-GCSs composite, as outlined in Table S1 (Supporting Information). The composite demonstrates an average surface area and pore size of 18.1 m^2/g and 2.7 nm, respectively.

Figure 3 presents the Raman spectra of ideal ND-GCSs, Gr-rec, and ND-rec. In the spectra of Gr-rec (Figure 3a), two primary peaks, namely, the G band at 1579 cm^{-1} and the 2D band at 2717 cm^{-1} , were respectively observed. On the other hand, in the Raman spectra of ND-rec (Figure 3b), a prominent peak D-band appeared at approximately 1333 cm^{-1} , along with a smaller G-band peak centered at around 1555 cm^{-1} recorded. The Raman spectra of the ND-GCSs

(Figure 3c) displayed three unique peaks combining the two distinct mixed carbon material spectra at 1333, 1579, and 2717 cm^{-1} . Among these, the peaks at approximately 1579 cm^{-1} correspond to the G-band and 2717 cm^{-1} corresponded to the 2D-band of graphene, respectively, where the G-band signifies graphitic sp^2 bonding. The D-band attenuation in the graphene sample suggests the absence of structural defects and/or indicates minimal impurity, indicative of a high-order crystalline structure.²⁵

The novel synthesized ND-GCSs crystalline structures and phases and pure samples were further evaluated, as depicted in Figure 4a–c. The XRD patterns were indexed utilizing the International Centre for Diffraction Data with cards numbered 00-006-0675 and 01-089-8493, supplemented by findings from a previously published study.³³ The XRD patterns of the Gr-rec sample reveal diffraction peaks at approximately $2\theta = 25.3$ and 53.7° , consistent with the planes of graphite (002) and (004), respectively. The XRD patterns of ND-rec displayed different peaks corresponding to the diamond crystal planes [$2\theta = 25.4^\circ$ (002), 34.8° (004), 43.2° (111), 57.3° (103), and 74.9° (220), respectively]. The planes (004) and (002) in the ND-rec reveal the existence of the sp^2 structure.^{31,33} The new composite spheres' XRD patterns are compatible with a composite of both nanodiamond and graphene, and they also agreed with pure samples as well as the previous studies from the literature.^{33,34} The full width at half-maximum (fwhm) of XRD spectra from Gr-rec flakes and ND-GCSs composite was also determined as 0.67 and 0.74° , respectively. The ND-GCSs composite shows three peaks associated with graphene and NDs, as shown in Figure 4c. This indicates the formation of crystalline ND-GCSs derived from ND and graphene particles. The crystallite size was computed using the Scherrer equation defined as $L_s = \kappa\lambda/\beta_s \cos(\theta_B)$, where κ is a geometrical factor,

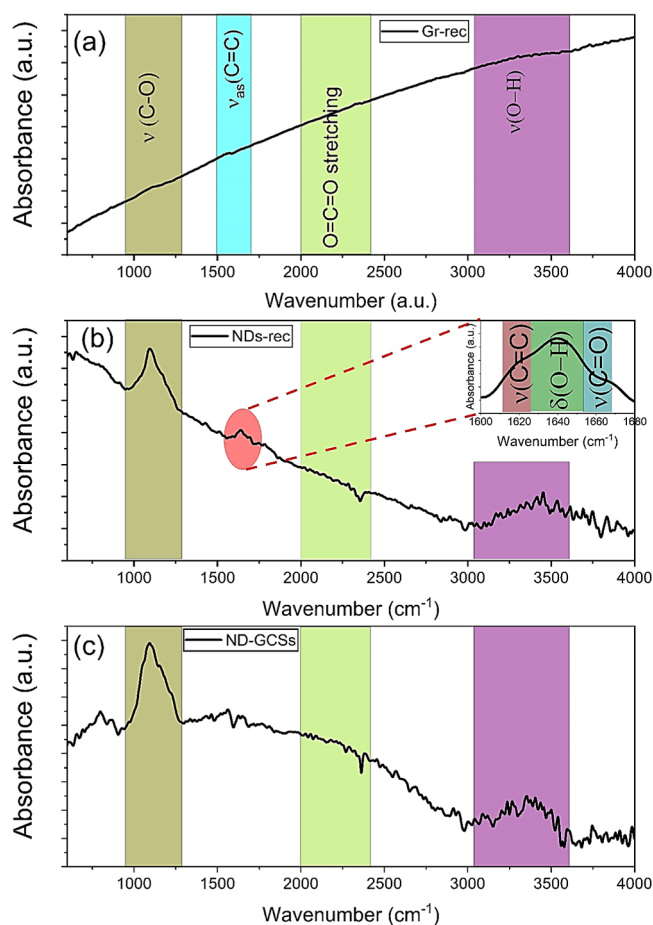


Figure 6. FTIR spectra of Gr-rec (a), ND-rec (b), and (c) optimized ND-GCSs.

λ is the X-ray wavelength, and θ_B Bragg angle, while β_s is the peak fwhm.³⁵ The crystallite size of ND-GCSs is found to be ~ 11.49 nm and that of the Gr-rec flakes is found to be ~ 12.69 nm, respectively.

The chemical states and carbon atomic percentages on the surfaces of both synthetic ND-DCSs pure samples were investigated by using XPS analyses, depicted in Figure 5a–d. The elemental chemical states of all of the carbon materials under this study are illustrated in Figure 5a. The existence of carbon (C) and oxygen (O) components was confirmed through the XPS analysis as expected. The XPS values for the CCSs sample indicated the percentage of the C element as

87.8% and that of the O element as 12.2%, respectively. Remarkably, no additional elements from either the used solvents or any other unforeseen impurities were detected. In Figure 5b, the Gr-rec C 1s peak exhibited two peaks at energies of approximately 284.83 and 285.98 eV, corresponding to sp^2 and sp^3 hybridization, respectively. Deconvolution analysis of the NDs-rec C 1s spectrum in Figure 5c revealed two peaks at 283.3 eV and approximately 285.5 eV, attributed to sp^2 hybridized C atoms and sp^3 , respectively.^{25,29} Further examination of the new composite spheres in Figure 5d indicated the presence of a hydroxy group (C–O) at an energy of approximately 287.2 eV. The findings further suggested that the amount of sp^2 bonds outweighs that of sp^3 bonds in the ND-GCSs, implying the ND-GCSs surface formation of graphene which is consistent with Raman and XRD findings.

FTIR was used to ascertain the chemical group functions of the ND-rec, Gr-rec, and Gr-NDs nanocomposite samples; the results are shown in Figure 6. As shown in Figure 6a–c, the synthesized ND-GCSs sample FTIR spectra, which included the starting components (Gr-rec and ND-rec), were recorded at room temperature in the 500–4000 cm^{-1} frequency range. FTIR analysis was employed to determine the chemical group functionalities of the ND-rec, Gr-rec, and Gr-NDs nanocomposite samples, as shown in Figure 6. FTIR analysis was utilized to determine the functional groups in the ND-GCSs and other pure carbon materials used herein; the results are depicted in Figure 6. As shown in Figure 6a–c, the synthesized ND-GCSs sample FTIR spectra, incorporating the initial components (Gr-rec and ND-rec), were obtained between the 500 and 4000 cm^{-1} frequency range. Initially, consistent with published FTIR data on Gr, the Gr-rec sample's spectrum exhibits bands that are challenging to discern.^{29,36} However, a narrow band is discernible in the ~ 1650 to 1500 cm^{-1} range and centered around 1572 cm^{-1} , attributed to the asymmetric stretch of sp^2 -hybridized C=C within the Gr structure. Figure 6b displays an absorption peak position at 1094 cm^{-1} , assigned to the C–O stretching mode. A diminished bandwidth (~ 3200 to 3450 cm^{-1}) typically signifies the OH stretching vibration mode of water, reflecting the presence of minor water clusters.²⁹ The NDs-rec FTIR spectrum depicts a weak band coupled with two shoulders within the 1600 – 680 cm^{-1} region and positions at 1665 cm^{-1} attributed to C=C stretching mode, 1640 cm^{-1} assigned to OH bending mode, and 1620 cm^{-1} C–C stretching vibration, respectively.³⁶ Remarkably, no additional peaks are recorded in the novel ND-GCSs

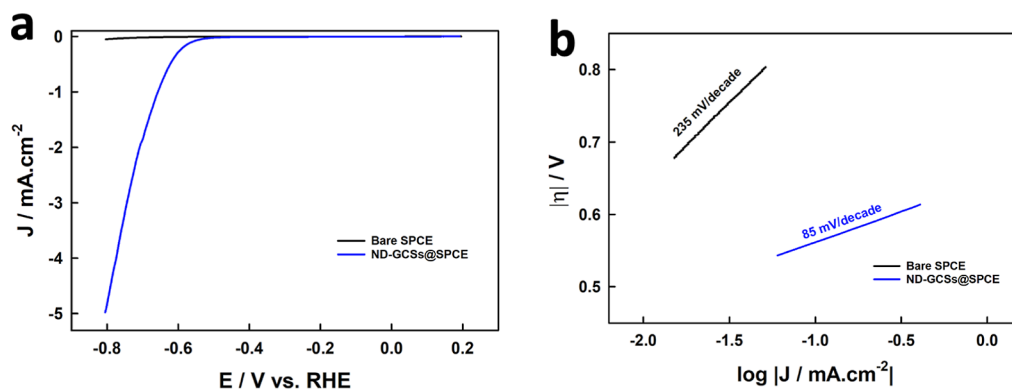


Figure 7. (a) LSV in a 0.5 M H_2SO_4 solution at bare SPCE and ND-GCSs@SPCE electrodes. (b) Tafel plots derived from the LSV data.

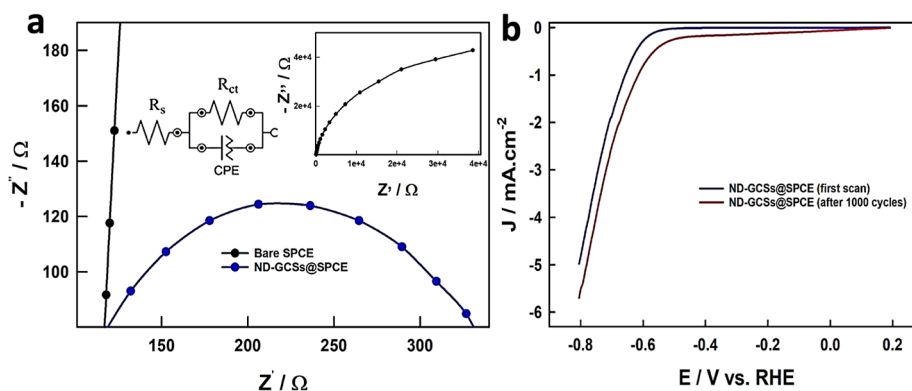


Figure 8. (a) EIS of bare SPCE and ND-GCSs@SPCE electrodes (a larger presentation of bare SPCE data is shown in the inset). (b), HER stability test of the ND-GCSs@SPCE electrocatalyst before and after 1000 cycles (at the same experimental conditions of Figure 7a).

Table 1. ICP Analysis of Optimized ND-GCSs, Produced Using Microwave Irradiation in a 1:1 Ratio of Xylene and DMF as the Solvents under Microwave Irradiation^a

element	concentration (in water) mg/L	concentration (in acid digestion) (mg/g)
Pt	BDL	0.002
Pd	BDL	0.014
W	BDL	0.006
Mo	0.006	0.066
Fe	0.226	0.17
Ni	0.048	0.124
Cr	0.033	0.04
Co	0.09	0.09
Cu	0.024	0.186
Mn	0.027	0.157
Ti	BDL	0.005
V	0.015	0.127
Ru	BDL	0.002
Rh	BDL	0.004

^aBDL: below the detection limit.

composite, indicating the removal of solvent residue from the nanocomposite material.

3.2. Electrocatalysis of HER. The electrochemical performance of the prepared ND-GCSs toward the electrocatalysis of HER was first evaluated using LSV as shown in Figure 7a. It can be noted that, while bare SPCE has practically no detectable HER activity, the ND-GCSs modified electrode presents a clear catalytic activity expressed as a relatively low onset potential of ca. -450 mV. Moreover, the extracted Tafel Plots are displayed in Figure 7b. This is typically used to illustrate the reaction mechanism, the rate-determining step, and the reaction kinetics of the electrocatalyst toward the HER. The plots obey the Tafel equation $\eta = a + b \log j$, where η is the overpotential, a is the Tafel constant, b is the Tafel slope and j is the current density. The calculated Tafel slopes reveal a clear decrease from about 235 to about 85 mV/decade between bare SPCE and the prepared ND-GCSs@SPCE catalyst. This observation supports the positive catalytic activity of the prepared electrocatalyst toward HER.

Further investigation of the interfacial reactions and electrocatalytic kinetics of the ND-GCSs@SPCE during the HER were carried out by EIS, as shown in Figure 8a, as Nyquist plots representation of both bare SPCE and ND-GCSs@SPCE electrocatalyst. The experimental data fitting was based on the Randles equivalent circuit (given in the same

figure). An excellent enhancement of the electron transfer kinetics is proven by the drastic decrease of the charge transfer resistance (R_{ct}) from 98.4 k Ω at bare SPCE to as low as 265 Ω for ND-GCSs@SPCE.

Along with its remarkable electrocatalytic activity, stability is an important aspect to consider when evaluating HER catalysts. For this, CV measurement was employed to further evaluate the stability of the prepared ND-GCSs@SPCE electrocatalyst. A continuous 1000 potential cycle in 0.5 M H_2SO_4 was imposed. The comparison of the LSV results before and after this excessive cycling is given in Figure 8b. An eye-catching feature is the slightly reduced current densities, which proves the excellent long-term stability of our ND-GCSs@SPCE electrocatalyst. As per existing literature, numerous graphene-encapsulated metals and metal alloy nanoparticles have been investigated to enhance the hydrogen evolution reaction (HER). Table S2 presents the electrochemical parameters of ND-GCSs in comparison with various materials.^{37–40} Furthermore, a thorough metal analysis using ICP on the optimized ND-GCSs was performed to verify the purity of the produced composite and determine the presence of some metals that may have influenced the HER performance of the produced composite, as presented in Table 1. The concentration of the analyzed metals was all found to be within a negligible range that may not have a significant influence on the recorded HER performance.

4. CONCLUSIONS

In summary, diamond nanoparticles assisted the exfoliation of graphite into a few layers of graphene and conversion into uniform composite spheres using micromixing. The fabricated ND-GCSs are highly uniform in their shape and size, particularly after the initial treatment by high-power ultrasonication. These attractive highly uniform composite carbon sphere products were obtained at optimal growth conditions using the microwave technique, e.g., at 1000 W for 30 min, with a composition of 95% graphene and 5% NDs. The synthesized ND-GCSs nanocomposite catalysts showed interesting catalytic performance for HER in an acidic media with a significant shift of the onset potential to ca. -450 mV and ca. 85 mV/decade Tafel slope of the prepared ND-GCSs@SPCE electrocatalyst. This was further supported by a tremendous decrease in charge transfer resistance to ca. 265 Ω , showing an enhanced electron transfer. Furthermore, the prepared electrocatalyst showed excellent long-term stability.

■ ASSOCIATED CONTENT

Data Availability Statement

All underlying data are available in the article itself and its Supporting Information.

SI Supporting Information

The Supporting Information is available free of charge at <https://pubs.acs.org/doi/10.1021/acsomega.3c06718>.

Additional information on control experiments and optimizing conditions for fabricating and controlling the ND-GCSs; BET analysis was also conducted on the optimized ND-GCSs composite; and electrochemical parameters of ND-GCSs compared with different materials from the literature (PDF)

■ AUTHOR INFORMATION

Corresponding Authors

Ibrahim K. Alsulami – Department of Science, King Abdulaziz Military Academy (KAMA), Riyadh 13959, Saudi Arabia; Centre of Nanotechnology and K. A. CARE Energy Research and Innovation Centre, King Abdulaziz University, Jeddah 21589, Saudi Arabia; Email: dralsulami2@gmail.com

Shittu Abdullahi – Centre of Nanotechnology and Physics Department, Faculty of Science, King Abdulaziz University, Jeddah 21589, Saudi Arabia; Department of Physics, Faculty of Science, Gombe State University, Gombe 760214, Nigeria; orcid.org/0000-0002-7010-4628; Email: shittub2k@gmail.com

Numan Salah – Centre of Nanotechnology and K. A. CARE Energy Research and Innovation Centre, King Abdulaziz University, Jeddah 21589, Saudi Arabia; orcid.org/0000-0002-8233-7373; Email: nsalah@kau.edu.sa

Authors

Ahmed Alshahrie – Centre of Nanotechnology and Physics Department, Faculty of Science, King Abdulaziz University, Jeddah 21589, Saudi Arabia

Thaar M. D. Alharbi – Physics Department, Faculty of Science, & Nanotechnology Centre, Taibah University, Al Madinah Al Munawwarah 42353, Saudi Arabia

Mohammed Alahmadi – Chemistry Department, College of Science, Taibah University, Al-Madinah Al-Munawwarah 42353, Saudi Arabia

Sami B. E. N. Aoun – Chemistry Department, College of Science, Taibah University, Al-Madinah Al-Munawwarah 42353, Saudi Arabia

Complete contact information is available at:

<https://pubs.acs.org/doi/10.1021/acsomega.3c06718>

Notes

The authors declare no competing financial interest.

■ ACKNOWLEDGMENTS

The authors gratefully acknowledge the financial support provided by KACARE-KAU Research Fellowship Program for the Post-Graduate Students.

■ REFERENCES

(1) Liu, X.; Zheng, H.; Sun, Z.; Han, A.; Du, P. Earth-Abundant Copper-Based Bifunctional Electrocatalyst for Both Catalytic Hydrogen Production and Water Oxidation. *ACS Catal.* **2015**, *5* (3), 1530–1538.

(2) Brisard, G. M.; Zenati, E.; Gasteiger, H. A.; Marković, N. M.; Ross, P. N. Ex Situ Low-Energy Electron Diffraction and Auger Electron Spectroscopy and Electrochemical Studies of the Underpotential Deposition of Lead on Cu(100) and Cu(111). *ACS Symp. Ser.* **1997**, *656* (100), 142–155.

(3) Brisard, G.; Bertrand, N.; Ross, P. N.; Marković, N. Oxygen Reduction and Hydrogen Evolution-Oxidation Reactions on Cu(Hkl) Surfaces. *J. Electroanal. Chem.* **2000**, *480* (1–2), 219–224.

(4) Qian, G.; Chen, J.; Luo, L.; Yu, T.; Wang, Y.; Jiang, W.; Xu, Q.; Feng, S.; Yin, S. Industrially Promising Nanowire Heterostructure Catalyst for Enhancing Overall Water Splitting at Large Current Density. *ACS Sustain. Chem. Eng.* **2020**, *8* (32), 12063–12071.

(5) Shen, F.; Wang, Y.; Qian, G.; Chen, W.; Jiang, W.; Luo, L.; Yin, S. Bimetallic Iron-Iridium Alloy Nanoparticles Supported on Nickel Foam as Highly Efficient and Stable Catalyst for Overall Water Splitting at Large Current Density. *Appl. Catal., B* **2020**, *278* (July), 119327.

(6) Xu, F.; Lu, J.; Luo, L.; Yu, C.; Tang, Z.; Abbo, H. S.; Titinchi, S. J. J.; Zhu, J.; Kang Shen, P.; Yin, S. Cu 2 S-Cu 3 P Nanowire Arrays Self-Supported on Copper Foam as Boosting Electrocatalysts for Hydrogen Evolution. *Energy Technol.* **2019**, *7* (4), 1800993.

(7) Yu, T.; Xu, Q.; Qian, G.; Chen, J.; Zhang, H.; Luo, L.; Yin, S. Amorphous CoO_x-Decorated Crystalline RuO₂ Nanosheets as Bifunctional Catalysts for Boosting Overall Water Splitting at Large Current Density. *ACS Sustain. Chem. Eng.* **2020**, *8* (47), 17520–17526.

(8) Xu, F.; Qian, G.; Chen, W.; Luo, L.; Shen, F.; Yin, S. Copper-Iron Selenides Ultrafine Nanowires as Cost-Effective Catalysts for the Oxygen Evolution Reaction at Large-Current-Density. *J. Phys. Chem. C* **2020**, *124* (36), 19595–19602.

(9) Morales-Guio, C. G.; Stern, L. A.; Hu, X. Nanostructured Hydrotreating Catalysts for Electrochemical Hydrogen Evolution. *Chem. Soc. Rev.* **2014**, *43* (18), 6555–6569.

(10) Chen, L.; Dong, X.; Wang, Y.; Xia, Y. Separating Hydrogen and Oxygen Evolution in Alkaline Water Electrolysis Using Nickel Hydroxide. *Nat. Commun.* **2016**, *7* (1), 11741–11748.

(11) Yu, C.; Xu, F.; Luo, L.; Abbo, H. S.; Titinchi, S. J. J.; Shen, P. K.; Tsiakaras, P.; Yin, S. Bimetallic Ni-Co Phosphide Nanosheets Self-Supported on Nickel Foam as High-Performance Electrocatalyst for Hydrogen Evolution Reaction. *Electrochim. Acta* **2019**, *317*, 191–198.

(12) Huang, K. J.; Zhang, J. Z.; Fan, Y. One-Step Solvothermal Synthesis of Different Morphologies CuS Nanosheets Compared as Supercapacitor Electrode Materials. *J. Alloys Compd.* **2015**, *625*, 158–163.

(13) Justin Raj, C.; Prabakar, K.; Dennyson Savariraj, A.; Kim, H. J. Surface Reinforced Platinum Counter Electrode for Quantum Dots Sensitized Solar Cells. *Electrochim. Acta* **2013**, *103*, 231–236.

(14) Hosseini, S. E.; Wahid, M. A. Hydrogen Production from Renewable and Sustainable Energy Resources: Promising Green Energy Carrier for Clean Development. *Renew. Sustain. Energy Rev.* **2016**, *57*, 850–866.

(15) Acar, C.; Dincer, I.; Naterer, G. F. Review of Photocatalytic Water-Splitting Methods for Sustainable Hydrogen Production. *Int. J. Energy Res.* **2016**, *40* (11), 1449–1473.

(16) Wang, S.; Lu, A.; Zhong, C. J. Hydrogen Production from Water Electrolysis: Role of Catalysts. *Nano Convergence* **2021**, *8* (1), 4.

(17) Yang, F.; Kang, N.; Yan, J.; Wang, X.; He, J.; Huo, S.; Song, L. Hydrogen Evolution Reaction Property of Molybdenum Disulfide/Nickel Phosphide Hybrids in Alkaline Solution. *Metals* **2018**, *8* (5), 359.

(18) Liu, X.; Dai, L. Carbon-Based Metal-Free Catalysts. *Nat. Rev. Mater.* **2016**, *1* (11), 16064.

(19) Zhu, Y.; Murali, S.; Cai, W.; Li, X.; Suk, J. W.; Potts, J. R.; Ruoff, R. S. Graphene and Graphene Oxide: Synthesis, Properties, and Applications. *Adv. Mater.* **2010**, *22* (35), 3906–3924.

(20) Xiang, Q.; Yu, J.; Jaroniec, M. Graphene-Based Semiconductor Photocatalysts. *Chem. Soc. Rev.* **2012**, *41* (2), 782–796.

- (21) Sarwar, S.; Nautiyal, A.; Cook, J.; Yuan, Y.; Li, J.; Uprety, S.; Shahbazian-Yassar, R.; Wang, R.; Park, M.; Bozack, M. J.; Zhang, X. Facile Microwave Approach towards High Performance MoS₂/Graphene Nanocomposite for Hydrogen Evolution Reaction. *Sci. China Mater.* **2020**, *63* (1), 62–74.
- (22) Bhaskar, A.; Deepa, M.; Rao, T. N.; Varadaraju, U. V. Enhanced Nanoscale Conduction Capability of a MoO₂/Graphene Composite for High Performance Anodes in Lithium Ion Batteries. *J. Power Sources* **2012**, *216*, 169–178.
- (23) Liu, Z.; Zhang, L.; Poyraz, S.; Smith, J.; Kushvaha, V.; Tippur, H.; Zhang, X. An Ultrafast Microwave Approach towards Multi-Component and Multi-Dimensional Nanomaterials. *RSC Adv.* **2014**, *4* (18), 9308–9313.
- (24) Kumar, R.; Sahoo, S.; Tan, W. K.; Kawamura, G.; Matsuda, A.; Kar, K. K. Microwave-Assisted Thin Reduced Graphene Oxide-Cobalt Oxide Nanoparticles as Hybrids for Electrode Materials in Supercapacitor. *J. Energy Storage* **2021**, *40* (March), 102724.
- (25) Kumar, R.; Sahoo, S.; Joanni, E.; Singh, R. K.; Kar, K. K. Microwave as a Tool for Synthesis of Carbon-Based Electrodes for Energy Storage. *ACS Appl. Mater. Interfaces* **2022**, *14*, 20306–20325.
- (26) Vejpravová, J. Graphene-Diamond Nanomaterials: A Status Quo Review. *Nanomaterials* **2021**, *11*, 2469.
- (27) Perevedentseva, E.; Lin, Y. C.; Cheng, C. L. A Review of Recent Advances in Nanodiamond-Mediated Drug Delivery in Cancer. *Expert Opin. Drug Delivery* **2021**, *18* (3), 369–382.
- (28) Bisht, A.; Samant, S. S.; Jaiswal, S.; Dasgupta, K.; Lahiri, D. Quantifying Nanodiamonds Assisted Exfoliation of Graphene and Its Effect on Toughening Behaviour of Composite Structure. *Composites, Part A* **2020**, *132* (November 2019), 105840.
- (29) Vejpravová, J. Mixed Sp²-Sp³ Nanocarbon Materials: A Status Quo Review. *Nanomaterials* **2021**, *11*, 2469.
- (30) Banerjee, D.; Sankaran, K. J.; Deshmukh, S.; Ficek, M.; Bhattacharya, G.; Ryl, J.; Phase, D. M.; Gupta, M.; Bogdanowicz, R.; Lin, I. N.; Kanjilal, A.; Haenen, K.; Roy, S. S. 3D Hierarchical Boron-Doped Diamond-Multilayered Graphene Nanowalls as an Efficient Supercapacitor Electrode. *J. Phys. Chem. C* **2019**, *123* (25), 15458–15466.
- (31) Alsulami, I. K.; Saeed, A.; Abdullahi, S.; Alshahrie, A.; Salah, N. Nanodiamonds as a Knife for Cutting Graphene Multilayers into Ultrafine Pieces under Microwave Irradiation. *FlatChem* **2022**, *36*, 100432.
- (32) Alsulami, I. K.; Saeed, A.; Abdullahi, S.; Hammad, A. H.; Alshahrie, A.; Salah, N. Microwave Irradiation for the Production of Graphene-Nanodiamond Composite Carbon Spheres. *Diam. Relat. Mater.* **2022**, *130*, 109411.
- (33) Wang, C.; Sun, X.; Li, H.; Liu, J.; Cheng, S.; Li, H.; Yuan, X. Hybrid TiO₂/Graphite/Nanodiamond Anode for Realizing High Performance Lithium Ion Battery. *ChemistrySelect* **2021**, *6* (7), 1458–1465.
- (34) Rajeevan, S.; John, S.; George, S. C. The Effect of Poly(Vinylidene Fluoride) Binder on the Electrochemical Performance of Graphitic Electrodes. *J. Energy Storage* **2021**, *39* (January), 102654.
- (35) Valério, A.; Morelhão, S. L. Usage of Scherrer's Formula in X-Ray Diffraction Analysis of Size Distribution in Systems of Monocrystalline Nanoparticles. *arXiv* **2019**, arXiv:1911.00701.
- (36) Alsulami, I. K.; Jilani, A.; Alshahrie, A.; Abdullahi, S.; Alharbi, T. M. D.; Gamal, A.; Moussa, M.; Salah, N. Fabrication of Highly Uniform Spherical Carbon Nanocomposite at Ultra-High Yield and Their Evaluation for Supercapacitor Application. *J. Mater. Res.* **2024**, *39*, 342–354.
- (37) Yang, L.; Liu, P.; Li, J.; Xiang, B. Two-Dimensional Material Molybdenum Disulfides as Electrocatalysts for Hydrogen Evolution. *Catalysts* **2017**, *7* (10), 285.
- (38) Devadas, B.; Imae, T. Hydrogen Evolution Reaction Efficiency by Low Loading of Platinum Nanoparticles Protected by Dendrimers on Carbon Materials. *Electrochem. Commun.* **2016**, *72*, 135–139.
- (39) Khadry, N. H.; Ghanem, M. A. Highly Dispersed Platinum Nanoparticles Supported on Silica as Catalyst for Hydrogen Production. *RSC Adv.* **2014**, *4* (91), 50114–50122.
- (40) Tang, Y. J.; Wang, Y.; Wang, X. L.; Li, S. L.; Huang, W.; Dong, L. Z.; Liu, C. H.; Li, Y. F.; Lan, Y. Q. Molybdenum Disulfide/Nitrogen-Doped Reduced Graphene Oxide Nanocomposite with Enlarged Interlayer Spacing for Electrocatalytic Hydrogen Evolution. *Adv. Energy Mater.* **2016**, *6* (12), 1–7.